Available online at www.sciencedirect.com

ScienceDirect

ICT Express 10 (2024) 608–613

www.elsevier.com/locate/icte

Short-term photovoltaic power forecasting based on hybrid quantum gated recurrent unit

Seon-Geun Jeong[a], Quang Vinh Do[b], Won-Joo Hwang[a,*]

[a] *Department of Information Convergence Engineering, Center for Artificial Intelligence Research, Pusan National University, Yangsan 50612, Republic of Korea*

[b] *Wireless Communications Research Group, Faculty of Electrical and Electronics Engineering, Ton Duc Thang University, Ho Chi Minh City 70000, Viet Nam*

Received 8 September 2023; received in revised form 17 November 2023; accepted 15 December 2023
Available online 20 December 2023

Abstract

Photovoltaic power generation forecasting is crucial for energy management, smart grid construction, and energy markets. This study proposes a hybrid quantum–classical gated recurrent unit (HQGRU)-based framework for forecasting short-term photovoltaic power generation in a time-series manner. The HQGRU model uses a classical layer followed by a quantum embedding circuit to convert classical data into quantum data. Subsequently, variational quantum circuits are used for feature extraction. To demonstrate the performance of the proposed model, we used practical data on photovoltaic power generation and the weather in Busan, Republic of Korea. The results demonstrate the high accuracy of the proposed HQGRU model.

Keywords: Hybrid quantum-gated recurrent unit; Photovoltaic power forecasting; Variational quantum circuit

1. Introduction

Solar energy is a promising renewable energy resource that is expected to mitigate climate change impacts and greenhouse emissions [1]. With the rapid development of photovoltaic (PV) systems, PV power has become an essential component in smart grids [2]. However, owing to complex weather conditions such as precipitation, cloud movement, temperature, relative humidity, and wind speed, PV power systems face critical challenges, including randomness, fluctuation, and uncertainty [3]. These conditions affect the stability and quality of power grids. To avoid this problem, short-term PV power forecasting is necessary for grid operation.

Numerous solar power forecasting methods based on deep-learning models have been recently proposed. In particular, recurrent neural networks (RNNs) have been widely used for short-term PV power forecasting [4,5]. A deep long short-term memory (LSTM)-RNN model accurately forecasted the solar power output [5]. Although LSTM has a high prediction accuracy, this approach requires a long training time and numerous trainable parameters. Compared to LSTM, gated recurrent unit (GRU) can mitigate these issues [4]. In particular, GRU can be used to save computational costs and time when dealing with a large dataset (i.e., historical weather data).

With the potential of superior quantum computers, quantum machine learning (QML) has emerged as a potentially faster solution than its classical counterparts [6]. Quantum neural networks (QNNs) have numerically shown a considerably higher capacity and faster training ability than comparable classical feedforward neural networks [7]. A hybrid quantum–classical QML algorithm relying on a variational quantum circuit (VQC) has been recently studied for noisy intermediate-scale quantum (NISQ) devices [8]. Because QNNs often suffer from the barren plateaus, where the loss landscape is extremely flat, the parameter optimization is difficult [9]. The VQC-based algorithms can avoid the barren plateaus, guaranteeing trainability [10]. Furthermore, QML with VQC can overcome the performance of classical machine learning. In particular, a VQC-based quantum LSTM (QLSTM) was proposed for time-series forecasting [11]. It shows that QLSTM learns faster and converges more stably than its classical counterparts. However,

* Corresponding author.
E-mail addresses: wjdtjsrms11@pusan.ac.kr (S.-G. Jeong), dovinhquang@tdtu.edu.vn (Q.V. Do), wjhwang@pusan.ac.kr (W.-J. Hwang).

Peer review under responsibility of The Korean Institute of Communications and Information Sciences (KICS).

https://doi.org/10.1016/j.icte.2023.12.005

the QLSTM model follows the standard structure of classical LSTM methods. This implies that the QLSTM requires several parameters and a long training time.

This paper presents a novel hybrid quantum GRU framework (HQGRU) for short-term PV power forecasting. The HQGRU model uses a classical layer followed by a quantum embedding circuit to convert classical data into quantum data. The proposed method implements VQCs to extract features. Specifically, inspired by the quantum convolution neural networks [12], we constructed the VQC layer (VQCL) to fully extract quantum features.

The main contributions of this study are summarized as follows:

- We develop a novel HQGRU framework to forecast PV power generation. The proposed HQGRU is designed as a hybrid QML model. To the best of our knowledge, this study is the first to apply the quantum-inspired GRU method, i.e., hybrid quantum computing methods, to short-term PV power forecasting.
- We introduce classical input and output layers before and after VQCs. The classical input layer and quantum embedding layer (QEL) convert the classical data into quantum data and VQCs extract the quantum features. In particular, we benchmark a reduced version of optimal quantum circuits for general two-qubit gates [8]. Furthermore, we construct VQCs similar to the quantum convolutional layer. This structure enables the VQCs to fully extract the quantum feature.
- The proposed HQGRU model can reduce the number of quantum circuits and the number of trainable parameters compared to the linear-layer-enhanced QLSTM (L-QLSTM) [13]. The proposed model is practical because it is suitable for NISQ devices.
- Finally, we provide comprehensive simulation results verifying the effectiveness of the proposed HQGRU. The simulations considered real weather and PV power generation historical data of the Republic of Korea. The proposed model is compared with classical and quantum benchmarks such as LSTM, GRU, and L-QLSTM.

The remainder of this paper is organized as follows. In Section 2, we describe the background of the VQC for the hybrid approach and L-QLSTM. Section 3 introduces the proposed framework and HQGRU model; we describe a quantum convolutional filter (QCF) for constructing the VQCL. Simulation results are presented in Section 4. Finally, we conclude the study in Section 5.

2. Background

2.1. VQC for hybrid approach

VQC is a quantum circuit with trainable parameters optimized according to a cost function in an iterative manner using a classical algorithm. As shown in Fig. 1, the general VQC architecture relies on three major components: a QEL, a VQCL, and a measurement layer. The QEL with embedding circuits

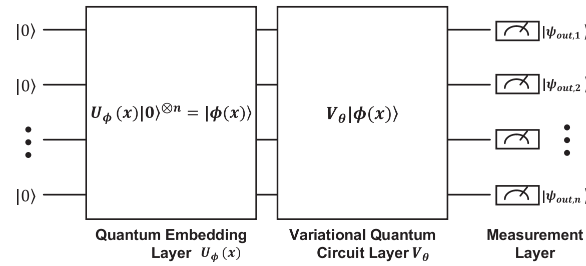

Fig. 1. General VQC architecture [8].

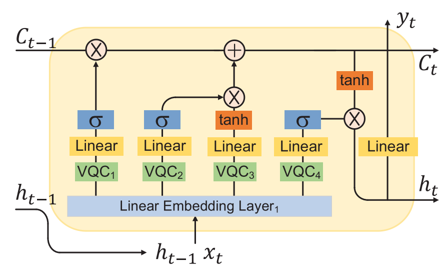

Fig. 2. Linear-layer-enhanced QLSTM model [13].

$U_\phi(x)$ converts the classical input data $x \in \mathbb{R}$ into quantum data $|\phi(x)\rangle$. The quantum state $|\phi(x)\rangle$ of the QEL inputs to the VQCL, and ansatz V_θ is applied to the VQCL, which is a trainable part containing parameterized quantum gate operations. The final output $|\psi\rangle = (|\psi_{\text{out},1}\rangle, |\psi_{\text{out},2}\rangle, \ldots, |\psi_{\text{out},n}\rangle)$ of the VQC is extracted from the measurement layer using Pauli operators.

2.2. Linear-layer-enhanced-QLSTM

L-QLSTM model is the hybrid quantum–classical version of the LSTM model. As shown in Fig. 2, L-QLSTM introduced a shared linear embedding layer before the VQCs and four separate linear layers after each VQC. The shared linear embedding layer converts the input data into the following VQCs, allowing compressing a feature of input data. The four separate linear layers remap the output of VQCs and enable the qubits to be adjusted freely. The corresponding forward-pass is as follows. First, the hidden state from the last timestep h_{t-1} and input features of the current timestep x_t are concatenated, which is passed to a linear embedding layer for transmitting into the four different VQCs. Subsequently, each outcome of VQCs is inputted to each linear layer, respectively. Finally, after following the specific activation functions, the results are connected and processed with different operations.

3. Methods

This study proposes an HQGRU framework for short-term PV power forecasting. In particular, we use practical data on the weather and PV power generation of Busan in the Republic of Korea. The proposed framework is shown in Fig. 3. The Korea Meteorological Administration (KMA) collects weather data such as precipitation, temperature, and relative humidity. The collected data are processed and managed at the data

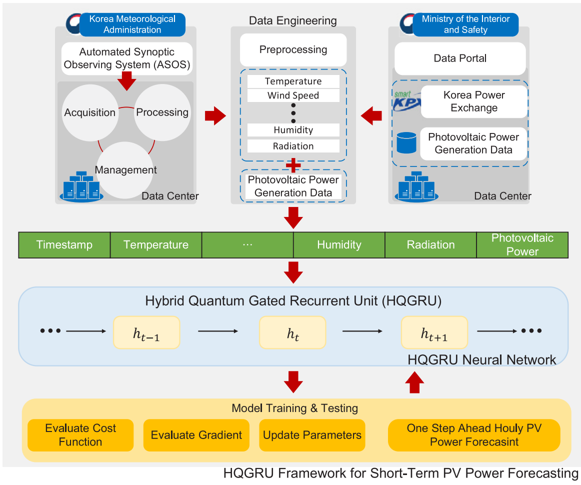

Fig. 3. Schematic illustration of the HQGRU framework for short-term PV power forecasting.

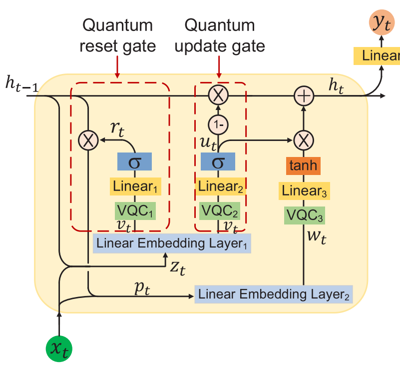

Fig. 4. Proposed HQGRU network.

center of KMA. The Ministry of the Interior and Safety (MIS) provides a Data Portal including PV power generation data from the Korea Power Exchange. We collected historical weather and PV power generation data for the target area from the KMA and MIS. We preprocessed the collected data by merging and removing null data. The preprocessed data were used as datasets to train and test the proposed HQGRU model.

3.1. Design of HQGRU

A classical GRU generally comprises reset and update gates. The reset gate controls the data measurements when new data are obtained. In contrast, the update gate continuously updates the state of the memory cell. Owing to this structure, the GRU consists of fewer parameters and fewer gates than LSTM. The proposed HQGRU shown in Fig. 4 was motivated by this architecture. That is, HQGRU comprises a quantum reset gate and a quantum update gate. Compared to the GRU, HQGRU replaces the classical neural networks in different gates with VQCs. This structure enables fewer parameters than GRU.

We introduce two linear embedding layers. The linear embedding layer prior to the VQC maps the input data into

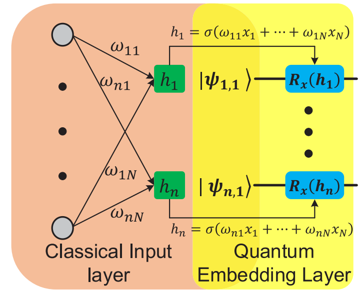

Fig. 5. Illustration of the hybrid embedding layer including the classical input layer and quantum embedding layer [8].

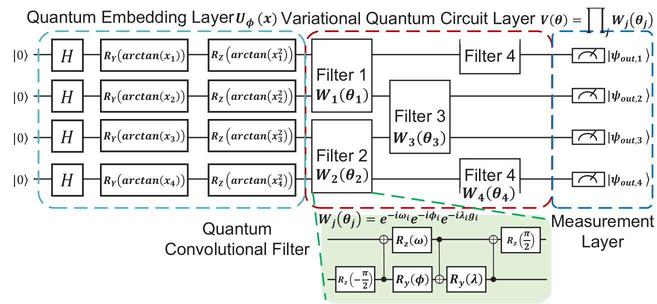

Fig. 6. VQC in the HQGRU model, where H, R represents a quantum gate, and x is the vector of classical input data. The implemented VQC is used as a quantum convolutional filter.

the rotation parameters of the QEL. Specifically, an angle-embedding scheme was used to construct the QEL $U_\phi(x)$. As shown in Fig. 5, the classical N-dimensional input vector $\mathbf{x} = [x_1, \ldots, x_N]^T$ is converted into the rotation angle of the quantum embedding circuits from the output of the classical input layer activations $[h_1, \ldots, h_n]^T$, where nth rotation angle can be represented as $h_n = \sigma(\omega_{n1}x_1 + \cdots + \omega_{nN}x_N)$, where $\sigma(\cdot)$ is the activation function. This changes the initial states $|\psi_{n,1}\rangle$ of the nth qubits as $|\psi_{n,2}\rangle = R_x(h_n)|\psi_{n,1}\rangle$. These encoded quantum states can be used as inputs for the subsequent VQCL.

The VQCL comprises a series of unitary operators. We benchmark the reduced version of optimized VQC as a QCF, as shown in Fig. 6 for constructing the VQCL, proposed in [8]. The VQCL ansatz $V(\theta)$ comprises multiple QCF $W_j(\theta)$: $V(\theta) \equiv \prod_{j=1} W_j(\theta_j)$, where θ_j is the variational parameters of jth VQC. Each QCF $W_j(\theta_j)$ can be expressed as an exponential with a nonparametric unitary $g_j = \sum_{k=1}^{K_j} \beta_{jk} P_k$, which can be any Hermitian operator on n qubits, where P_k is a string of Pauli matrices on n qubits, and β_{jk} is a constant for all j, k. Therefore, the QCF can be expressed as the product of the exponentials of each term: $W_j(\theta_j) = \prod_k e^{-i\theta_j \beta_{jk} P_k}$. In addition, the overall ansatz $U(\theta)$ can be represented as follows: $U(\theta) = U_\phi V(\theta)$. In the measurement layer, the expected values of the measured observables were as follows: $\langle \hat{B}_i \rangle = \langle x|U(\theta)^\dagger B_i U(\theta)|x\rangle$, where the observables $\hat{B}_i$ are typically Pauli-Z operators for one or more qubits. $\langle \hat{B}_i \rangle$ can be used as input to the following classical linear layer.

The forward-pass process is as follows: First, the hidden state from the last timestep h_{t-1} and the input features of the current timestep x_t are concatenated as z_t. Subsequently, z_t is passed to a linear embedding layer L_{e1} for transmitting into the rotation angle of QEL. Subsequently, the outcome v_t of L_{e1} passes through the quantum reset and quantum update gates. The outcomes r_t and u_t are calculated after computing VQC_1, VQC_2, linear layers L_1, L_2, and sigmoid activation σ. Outcomes r_t and h_{t-1} are concatenated and passed to a linear embedding layer L_{e2}. The outcome w_t of L_{e2} is then inputted to VQC_3. Finally, after applying the linear layer L_3 and the hyperbolic tangent $tanh$, h_t is calculated from the quantum update gate and the outcome of $tanh$. The formulae for the forward pass are as follows:

$$z_t = [h_{t-1}, x_t] \tag{1}$$

$$v_t = L_{e1}(z_t) \tag{2}$$

$$r_t = \sigma(L_1(VQC_1(v_t))) \tag{3}$$

$$u_t = \sigma(L_2(VQC_2(v_t))) \tag{4}$$

$$p_t = r_t \otimes h_{t-1} \tag{5}$$

$$w_t = L_{e2}(p_t) \tag{6}$$

$$h_t = tanh(L_3(VQC_3(w_t))) \otimes u_t + (1 - u_t) \otimes h_{t-1} \tag{7}$$

$$y_t = L_4(h_t) \tag{8}$$

where the subscript t denotes the time step. $[\cdot]$ represents vector concatenation. $\otimes$ denotes the Hadamard product (element-wise product), and y_t is the output. Circuit layer operations per second (CLOPS) is a metric correlated with how fast a quantum processor can execute circuits [14]. Therefore, the execution time $\hat{T}$ of a job consisting of M quantum circuits with an effective number of quantum volume layers D_{eff} on a system with CLOPS C for a total of S shots is represented as $\hat{T} = \frac{MS}{C} \times D_{eff}$. Compared to L-QLSTM, HQGRU has fewer quantum trainable parameters and fewer VQCs. Therefore, HQGRU requires less execution time than L-QLSTM. That is, this structure allows faster convergence than L-QLSTM and is suitable for NISQ devices.

3.2. Parameters learning of HQGRU

Using a gradient-based strategy, the gradient of the VQC can be represented by the parameter-shift rule as follows [13]:

$$\frac{\partial f(x,\theta)}{\partial \theta} = \frac{1}{2}\left[f(x, \theta + \frac{\pi}{2}) - f(x, \theta - \frac{\pi}{2})\right], \tag{9}$$

where $f(x, \theta)$ denotes the output with respect to the variational parameters θ and the input features x. The cost function L can be optimized by backpropagating the gradients between VQCs and classical layers iteratively, as summarized in Algorithm 1.

Algorithm 1 HQGRU-based short-term PV power forecasting algorithm

input : Training and test datasets $x, xt \in \mathcal{X}$, label $y, yt \in \mathcal{Y}$,trainable parameters θ, learning rate η, and the number of training epochs N
output: PV power generation forecasting one hour ahead

```
Build: Build the HQGRU model and set the parameters θ and the learning rate η.
Initialize: Initialize the hyper parameters in the VQCs and linear layers θ as well as the hidden state h0 to 0
Train HQGRU model
for n = 1 to N do
    Forecast short-term PV power ŷ by feeding x into the HQGRU model.
    Evaluate the cost function L between y and ŷ.
    Evaluate gradient ∂f(x,θ)/∂θ
    Update the trainable parameters θ in the VQCs and linear layers by backpropagation of the cost function L.
end
Test trained HQGRU (xt, yt)
PV power generation forecasting results one hour ahead
```

4. Experimental results

This section presents the simulation results demonstrating the effectiveness of the proposed HQGRU algorithm for short-term PV power forecasting. We used historical data such as temperature (°C), precipitation (mm), wind speed (m/s), relative humidity (%), duration of sunshine (h), solar irradiance (MJ/m^2), and PV power generation (MWh) of Busan in the Republic of Korea provided by KMA and the Data Portal of MIS. The historically measured time-series frames $(t-1), (t-2), (t-3), \ldots, (t-24)$ were used to forecast the future PV power (t). Specifically, the datasets contained a sampling resolution of 1 h from January 1, 2019, to March 31, 2020. A total of 80% of the datasets were used for training, and the remaining datasets were used for testing.

The proposed HQGRU algorithm was compared with LSTM, GRU, and L-QLSTM [13] as benchmarks to demonstrate its effectiveness. Considering the dimension of input data 6, HQGRU and L-QLSTM are 6-qubit models. Despite increasing the number of cells in the experiment, no significant performance improvement was observed. Therefore, we set the number of cells in the models to 32. Considering the convergence time, all models, were trained for 30 epochs. In consideration of memory, the batch size was set to one. The Adam optimizer was used with a learning rate of 10^{-3}, and the mean square error (MSE) was used as a loss function. All experiments were performed on a PC with an AMD Ryzen 5 5600G 6-core Processor CPU and 16 GB of RAM. The experiments were implemented using PyTorch1.0, and PennyLane [15].

To measure the performance of the algorithms, we adopted the mean absolute error (MAE), root mean square error (RMSE), and R-square (R^2), which are widely used evaluation metrics for prediction performance of the model [4,5].

Table 1
Performance of different algorithms, where Q represents the number of qubits.

Model	MAE	RMSE	R^2	Parameters
LSTM	1.336	2.391	0.959	5153
GRU	1.323	2.363	0.960	3873
L-QLSTM	1.367	2.383	0.959	1131+6Q
Proposed HQGRU	1.301	2.347	0.961	971+6Q

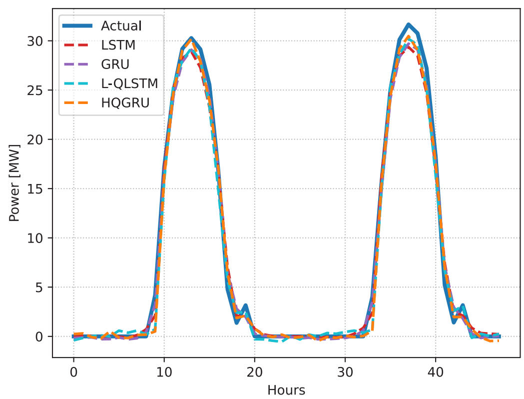

Fig. 7. Sample performance for 1-h forecasting horizons from 10 Jan 2020 to 12 Jan 2020.

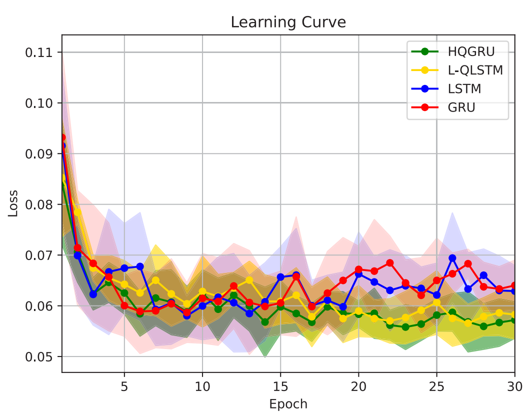

Fig. 8. Comparison of losses between LSTM, GRU, L-QLSTM, and HQGRU.

Table 1 shows performances of the proposed HQGRU and benchmarks, where the results were chosen for the top accuracy. From Table 1 and Fig. 7, HQGRU exhibits RMSE, MAE, and R^2 values of 2.347 MWh, 1.301 MWh, and 0.961, respectively. In contrast, R^2 values of the other benchmarks reached 0.959–0.960. These results indicate that the HQGRU model with the fewest parameters can achieve high accuracy.

Fig. 8 presents a comparison of the losses including standard deviations between the benchmarks and HQGRU. We can observe that the classical algorithm has faster convergence time for training loss regarding epochs. Due to the limited availability of open-access quantum backends, we have conducted the simulation of quantum algorithms on quantum computers up to 4 epochs. The results of quantum algorithms are obtained from classical computers. However, in an IBM quantum computer based on 7-qubit providing 2700-CLOPS, the training time of L-QLSTM and HQGRU per epoch is about 42 and 38 s, respectively. However, LSTM and GRU require about 59 s and 50 s per epoch, respectively. Therefore, HQGRU exhibited more convergence stability and faster convergence time than the benchmarks. In particular, the experimental results showed that HQGRU outperformed the L-QLSTM.

5. Conclusion

This paper proposes an HQGRU-based framework for short-term PV power forecasting. We used linear layers and QEL to transform classical data into quantum data while allowing flexible qubit usage. To construct the VQCL, we introduce the quantum convolutional layer concept. In particular, we benchmarked the reduced version of optimized VQC as a QCF. The effectiveness of the proposed HQGRU algorithm was verified by comparing it with benchmarks. The simulation results showed that HQGRU with the fewest number of parameters can achieve high accuracy for the target task. This study demonstrated that the proposed approach can be applied to sequential data using quantum-based algorithms. Especially, we expect that the proposed HQGRU could be used to develop information and communication technology to improve the stability and quality of power grids. In the current capacity of NISQ devices, hybrid QML structures, such as the proposed HQGRU, are powerful. This could be demonstrated by implementing the proposed HQGRU on a real quantum computer in future work.

CRediT authorship contribution statement

Seon-Geun Jeong: Conceptualization, Methodology, Implementation, Writing – original draft, Experiment. **Quang Vinh Do:** Validation, Writing – review & editing. **Won-Joo Hwang:** Supervision.

Declaration of competing interest

The authors declare that they have no known competing financial interests or personal relationships that could have appeared to influence the work reported in this paper.

Acknowledgment

This work was supported by a 2-Year Research Grant of Pusan National University, South Korea.

References

[1] Z. Xin-gang, Z. You, Technological progress and industrial performance: A case study of solar photovoltaic industry, Renew. Sustain. Energy Rev. 81 (2018) 929–936.
[2] E. Scolari, L. Reyes-Chamorro, F. Sossan, M. Paolone, A comprehensive assessment of the short-term uncertainty of grid-connected PV systems, IEEE Trans. Sustain. Energy 9 (3) (2018) 1458–1467.
[3] J. Hossain, A. Mahmud, Renewable Energy Integration: Challenges and Solutions, Springer Science & Business Media, 2014.
[4] Y. Wang, W. Liao, Y. Chang, Gated recurrent unit network-based short-term photovoltaic forecasting, Energies 11 (8) (2018) 2163.

[5] M. Abdel-Nasser, K. Mahmoud, Accurate photovoltaic power forecasting models using deep LSTM-RNN, Neural Comput. Appl. 31 (7) (2019) 2727–2740.

[6] C. Blank, D.K. Park, J.-K.K. Rhee, F. Petruccione, Quantum classifier with tailored quantum kernel, npj Quantum Inf. 6 (1) (2020) 41.

[7] A. Abbas, D. Sutter, C. Zoufal, A. Lucchi, A. Figalli, S. Woerner, The power of quantum neural networks, Nature Comput. Sci. 1 (6) (2021) 403–409.

[8] S.-G. Jeong, Q.-V. Do, H.-J. Hwang, M. Hasegawa, H. Sekiya, W.-J. Hwang, Hybrid quantum convolutional neural networks for UWB signal classification, IEEE Access 11 (2023) 113726–113739.

[9] Y. Liang, W. Peng, Z.-J. Zheng, O. Silvén, G. Zhao, A hybrid quantum–classical neural network with deep residual learning, Neural Netw. 143 (2021) 133–147.

[10] J.R. McClean, S. Boixo, V.N. Smelyanskiy, R. Babbush, H. Neven, Barren plateaus in quantum neural network training landscapes, Nat. Commun. 9 (1) (2018) 4812.

[11] S.Y.-C. Chen, S. Yoo, Y.-L.L. Fang, Quantum long short-term memory, in: ICASSP 2022 - 2022 IEEE International Conference on Acoustics, Speech and Signal Processing (ICASSP), 2022, pp. 8622–8626.

[12] I. Cong, S. Choi, M.D. Lukin, Quantum convolutional neural networks, Nat. Phys. 15 (12) (2019) 1273–1278.

[13] Y. Cao, X. Zhou, X. Fei, H. Zhao, W. Liu, J. Zhao, Linear-layer-enhanced quantum long short-term memory for carbon price forecasting, Quantum Mach. Intell. 5 (2) (2023) 1–12.

[14] T.L. Scholten, D.P.I. au2, J. Washington, J.R. Glick, T. Ward, A model for circuit execution runtime and its implications for quantum kernels at practical data set sizes, arXiv (2023) URL https://doi.org/10.48550/arXiv.2307.04980.

[15] V. Bergholm, J. Izaac, M. Schuld, C. Gogolin, S. Ahmed, V. Ajith, M.S. Alam, G. Alonso-Linaje, B. AkashNarayanan, A. Asadi, et al., PennyLane: Automatic differentiation of hybrid quantum-classical computations, arXiv (2022) URL https://doi.org/10.48550/arXiv.1811.04968.